Integrating nanohybrid membranes of reduced graphene oxide: chitosan: silica sol gel with fiber optic SPR for caffeine detection

2017 Nanotechnology 28 195502

(http://iopscience.iop.org/0957-4484/28/19/195502)

IOP Publishing Nanotechnology
Nanotechnology 28 (2017) 195502 (12pp) https://doi.org/10.1088/1361-6528/aa6a9c

Integrating nanohybrid membranes of reduced graphene oxide: chitosan: silica sol gel with fiber optic SPR for caffeine detection

Ravi Kant, Rana Tabassum and Banshi D Gupta

Physics Department, Indian Institute of Technology Delhi, New Delhi 110016, India

E-mail: bdgupta@physics.iitd.ac.in

Received 23 January 2017, revised 14 March 2017
Accepted for publication 31 March 2017
Published 19 April 2017

Abstract

Caffeine is the most popular psychoactive drug consumed in the world for improving alertness and enhancing wakefulness. However, caffeine consumption beyond limits can result in lot of physiological complications in human beings. In this work, we report a novel detection scheme for caffeine integrating nanohybrid membranes of reduced graphene oxide (rGO) in chitosan modified silica sol gel (rGO: chitosan: silica sol gel) with fiber optic surface plasmon resonance. The chemically synthesized nanohybrid membrane forming the sensing route has been dip coated over silver coated unclad central portion of an optical fiber. The sensor works on the mechanism of modification of dielectric function of sensing layer on exposure to analyte solution which is manifested in terms of red shift in resonance wavelength. The concentration of rGO in polymer network of chitosan and silica sol gel and dipping time of the silver coated probe in the solution of nanohybrid membrane have been optimized to extricate the supreme performance of the sensor. The optimized sensing probe possesses a reasonably good sensitivity and follows an exponentially declining trend within the entire investigating range of caffeine concentration. The sensor boasts of an unparalleled limit of detection value of 1.994 nM and works well in concentration range of 0–500 nM with a response time of 16 s. The impeccable sensor methodology adopted in this work combining fiber optic SPR with nanotechnology furnishes a novel perspective for caffeine determination in commercial foodstuffs and biological fluids.

Keywords: caffeine, reduced graphene oxide, chitosan, silica sol gel, surface plasmon resonance, optical fiber, sensor

(Some figures may appear in colour only in the online journal)

1. Introduction

Caffeine is an alkaloid belonging to the class of N-methyl xanthine compounds which naturally occur in tea leaves, cocoa beans, coffee beans and several other plants. In plants, caffeine is believed to act as a natural pesticide which inhibits insect feeding [1]. Being one of the chief constituents of commonly used beverages such as coffee, tea, soft and energy drinks caffeine is the most popular psychoactive drug consumed in the world. Identified chemically as 1, 3, 7-trimethylxanthine, caffeine forms an important component of several medications and used in the pharmacological formulation of analgesics in combination with other drugs such as paracetamol [2, 3]. A moderate consumption of caffeine improves alertness and work efficiency in addition to enhancing wakefulness by stimulating the central nervous system. However, high amount of caffeine could lead to various harmful effects such as nausea, trembling, nervousness and seizures in human body when consumed on regular basis [4]. Caffeine increases blood pressure by acting as a vasoconstrictor. It is also considered as a risk factor for cardiovascular diseases as it is found to be partially responsible

for increase in homocysteine concentration in human plasma [5]. Caffeine is implicated to influence several cellular processes in different organisms including plants, fungi and mammals at the cellular level [6]. Moreover, the rate of metabolism of caffeine by liver could uncover information about several critical and chronic diseases in addition to estimating their level of severity [7]. Due to these reasons, an accurate, sensitive, rapid and cost-effective detection methodology for caffeine is highly demanded from clinical point of view as well as to check the unwarranted usage of caffeine in commonly used medicinal and food products.

Numerous techniques and analytical procedures have been developed for caffeine determination in various matrix environments including biological fluids, pharmaceutical formulations, plants and commercial food products. These include chromatography [8–10], voltammetry [11, 12], amperometry [13], fluorescence [14], spectrophotometry [15], potentiometry [16], electrospray ionization ion mobility spectrometry [17], capillary electrophoresis [18] and electrochemical methods [19–22]. However, these methods turn out to be expensive and time consuming due to complex fabrication designs, longer duration and complicated steps for pretreatment and extraction of samples, involvement of lot of chemicals and instrumentation and mediocre stability and reproducibility.

In recent years, surface plasmon resonance (SPR) has emerged as a distinguished optical technique in the avenue of sensor technology and due to its various advantages research activities in the direction of SPR based fiber optic sensors have expanded considerably. Some prominent examples include the detection of activation of living cells [23], *in vivo* recording of neural activity for investigating neurons and their networks [24] and study of DNA hybridization and DNA-protein interactions [25]. A surface plasmon wave represents the TM polarized coherent charge density oscillations that propagate along a metal dielectric interface satisfying a resonance condition. The basic SPR based fiber optic sensor configuration involves removal of cladding from a small middle portion of an optical fiber which is further coated with a layer of plasmonic metal [26, 27]. An evanescent wave is generated at the core metal interface upon illumination of one end of the fiber with a polychromatic light source, which leads to the excitation of surface plasmon wave at the interface encompassing metal and dielectric sensing medium. Maximum transfer of energy to surface plasmon wave occurs when the wave vectors of evanescent wave exactly coincides with that of the surface plasmon wave. This is manifested in terms of a sharp dip in the intensity of transmitted spectrum at a specific wavelength, termed as the resonance wavelength which depends on the dielectric constant of the sensing medium. Introduction of an over-layer of high refractive index material in the form of nanostructures over plasmonic metal layer in the fiber optic sensor configuration further augment the sensitivity of SPR based fiber optic sensors. A higher surface area to volume ratio furnished by nanostructures enhances the interaction of analyte molecules with the sensing layer in comparison to bulk material resulting in boosting the sensitivity. Various nanostructures in the form of nanoparticles, nanorods, nanoflowers, nanowires and nanospheres have been used in SPR based fiber optic sensors for sensing applications encompassing plenty of chemicals and biomolecules [28–31].

Since its characterization [32], graphene has attracted significant worldwide attention among the scientific community due to its amazing properties [33] and thus, finds extensive applications in different avenues such as biosensors [34], field-effect transistors [35], supercapacitors [36] and energy storage [37]. Furthermore, various oxidized and reduced forms of graphene derived through several physical and chemical protocols are also used for diverse applications. Among them, reduced graphene oxide (rGO) has turned up as a pioneer two-dimensional carbon nanomaterial attributable to its remarkable properties including high surface area, mechanical stability and ease of processing combined with tailored electrical and optical properties [38–40]. Moreover, rGO facilitates a pathway for loading of nanostructures such as metal nanoparticles providing them with an improved specific surface area which supports the use of rGO for sensing applications [41]. It also offers an alternative to produce great quantities of graphene sheets in solution phase. In addition, rGO exhibits excellent biocompatibility which benefits the modification and immobilization of biomolecules. Numerous biosensor designs based on rGO have been reported in the literature [42–44]. Further avenues for the design of potential biosensors are explored using a nanocomposite of rGO functionalized in a polymer matrix. Such nanocomposites synergistically combine the properties of polymers with distinct features of rGO which turn out to be favorable for sensing applications [45–47]. Recently, a study making use of rGO@polydopamine composite for the amperometric detection of chlorpromazine has been reported which displays good analytical sensitivity and substantially good stability and reproducibility [48]. In view of above, a nanohybrid arrangement of rGO functionalized in an appropriate polymer matrix presents itself as an ideal candidate for designing of biosensors.

In this study, we report the implementation of chemically synthesized nanohybrid membrane of rGO encapsulated in chitosan modified silica sol gel (rGO: chitosan: silica sol gel) as the sensing surface for the detection of caffeine. The hybrid network of chitosan modified silica sol gel has been employed as a supporting framework for the fabrication of SPR based fiber optic caffeine sensor. In addition to providing mechanical flexibility, the hydrophobicity and the porosity of this hybrid network can be tuned appropriately to overcome the limitations incurred due to the use of a single material for fabrication such as the brittleness of inorganic materials and the swelling of polymers [49, 50]. Furthermore, chitosan exhibits fantastic film-forming capability, superior adhesive nature and non-toxicity with a propensity to chemical modification. The morphological investigation of the synthesized rGO: chitosan: silica sol gel nanohybrid membrane has been explored through SEM. The sensing layer has been exercised over the silver coated unclad region of an optical fiber through dip coating technique. The fabricated sensor has been characterized through the spectral interrogation mode and a

red shift in the resonance wavelength with an increase in caffeine concentration has been observed. The optimization of experimental variables such as the concentration of rGO being encapsulated in hybrid network of chitosan modified silica sol gel, dipping time of sensing probe in solution of rGO: chitosan: silica sol gel and pH of the buffer solution used for preparing caffeine solutions has been achieved through SPR studies. The present work combines the sensitivity and specificity of fiber optic SPR sensors with enhanced sensing characteristics of nanomaterials which load the sensor with enormous advantages apart from displaying its suitability for commercial applications for caffeine detection.

2. Experimental

2.1. Chemicals and materials

Plastic clad silica (PCS) optical fiber with 600 μm core diameter and 0.37 numerical aperture was purchased from Fiberguide Industries (USA). Caffeine, graphene oxide (GO), hydrazine hydrate, 3-mercaptopropyltrimethoxysilane (MPTMS) and chitosan were procured from Sigma Aldrich. Sodium acetate, acetic acid, sodium dihydrogen phosphate and disodium hydrogen phosphate were bought from Merck. Silver wire (99.99% purity) was purchased from a local vendor in Delhi. Deionizing water procured from Millipore® was used during experimentation and for preparing analyte solutions. All the chemicals were used as received without any further modification or purification.

2.2. Preparation of rGO: chitosan: silica sol gel nanohybrid membrane

A simple chemical route as described in [50] was followed for the preparation of rGO: chitosan: silica sol gel nanohybrid membrane. Acetate buffer (0.1 M, pH 5.0) was prepared by dissolving appropriate amount of sodium acetate in acetic acid. Then, chitosan solution was prepared by dissolving 0.2 g of chitosan in 100 ml acetate buffer solution under continuous stirring for 4 h. MPTMS, one of the silane-coupling agents, was selected as the cross-linking reagent to synthesize the hybrid network of chitosan silica sol gel. 10 ml of MPTMS was added drop wise in the chitosan solution to initiate the cross-linking reaction with the addition of few drops of HCl to complete the polymerization process. The mixture was then stirred for 6 h at 60 °C until a homogeneous solution was obtained. This way the chitosan modified silica sol gel was prepared.

A colloidal suspension of GO was prepared by dispersing 1 ml GO in 500 ml deionized water followed by ultrasonication for about an hour which was chemically reduced using hydrazine hydrate at 80 °C for 24 h to rGO [50, 51]. The resulting suspension was filtered and thoroughly rinsed with deionized water and ethanol followed by drying in oven to obtain rGO. Afterwards, an homogeneous suspension of rGO was prepared by dispersing 1 mg of rGO in 10 ml water and ultrasonicating for half an hour. This suspension was added to the prepared solution of chitosan modified silica sol gel to encapsulate rGO into the hybrid polymer matrix of chitosan modified silica sol gel. The resulting solution was stirred for 5 h to obtain a homogeneous solution. After cooling it down to room temperature, the solution was washed thoroughly with ethanol and deionized water to remove any trace of impurities left during the synthesis process. The final solution thus obtained was represented solution of rGO: chitosan: silica sol gel nanohybrid membrane. A schematic illustration of the steps followed for the synthesis of nanohybrid membrane of rGO: chitosan: silica sol gel is depicted in figure 1(a).

2.3. Fabrication of fiber optic sensing probe

To fabricate the fiber optic sensing probe, a 20 cm long PCS optical fiber was taken whose 1 cm central portion was unclad using a sharp blade. The unclad portion was cleaned first with acetone and then by ion bombardment inside a vacuum chamber kept at a pressure of 2–5 $\times$ 10^{-2} mbar. Thereafter, 40 nm thick layer of silver was deposited over 1 cm unclad core of the fiber optic probe using thermal evaporation coating unit (HIND HIVAC Model Number: 12A4D). The fiber optic probe was rotated to achieve the uniformity in the thickness of silver layer being deposited. The 40 nm thickness of the silver layer is the reported optimized thickness [52] at which more pronounced SPR curves are obtained. The thickness of the silver was monitored using a quartz crystal microbalance digital thickness monitor (with an accuracy of 0.1 nm) fixed in the coating unit. The deposition rate of silver was maintained at a constant rate of 0.04 nm s^{-1} to maintain the uniformity of the metal film being deposited. Subsequently, solution of rGO: chitosan: silica sol gel nanohybrid membrane was coated over the silver coated portion of the fiber optic probe using the dip coating technique. The prepared solution of nanohybrid membrane was ultrasonicated with deionized water for half an hour prior to its coating over the fiber optic probe. During dip coating, the probe was immersed into the solution of nanohybrid membrane and pulled out at a constant speed after some time. The time during which the probe was immersed into the solution of nanohybrid membrane plays a crucial role in deciding the thickness of the nanohybrid structure being deposited over the silver coated region. The adhesion of the nanohybrid structure over silver coated portion of the probe was achieved through high temperature annealing of the fiber for 8–10 h in an oven at 90 °C. This process also helps in reducing the permeability of the deposited nanohybrid layer towards liquid sample solutions. Figure 1(b) schematically illustrates the steps involved in the fabrication of the fiber optic sensing probe with multilayer of silver and rGO: chitosan: silica sol gel nanohybrid membrane. The schematic of the completely fabricated fiber optic sensing probe is displayed in figure 1(c).

2.4. Preparation of solutions

Calculated amounts of sodium dihydrogen phosphate and disodium hydrogen phosphate were dissolved in deionized water to prepare phosphate buffer solution of 0.1 M molarity

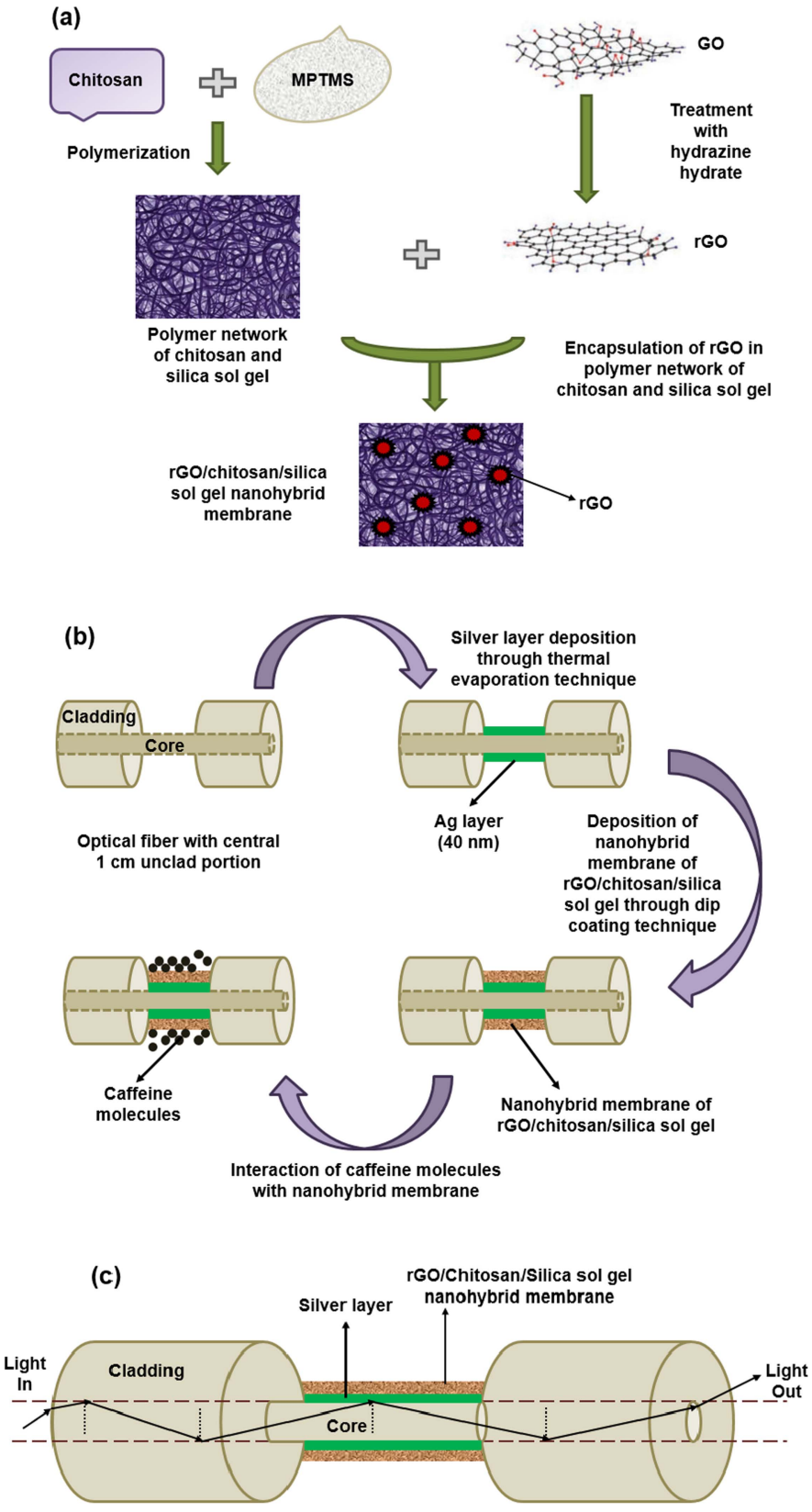

Figure 1. (a) Schematic representation of steps followed during the synthesis of nanohybrid membrane of rGO: chitosan: silica sol gel, (b) schematic illustrating fabrication steps of SPR based caffeine sensor comprising of multilayers of Ag (40 nm) and rGO/silica sol gel nanohybrid membrane over unclad core region of the optical fiber, (c) schematic of the complete fabricated fiber optic SPR probe showing different layers.

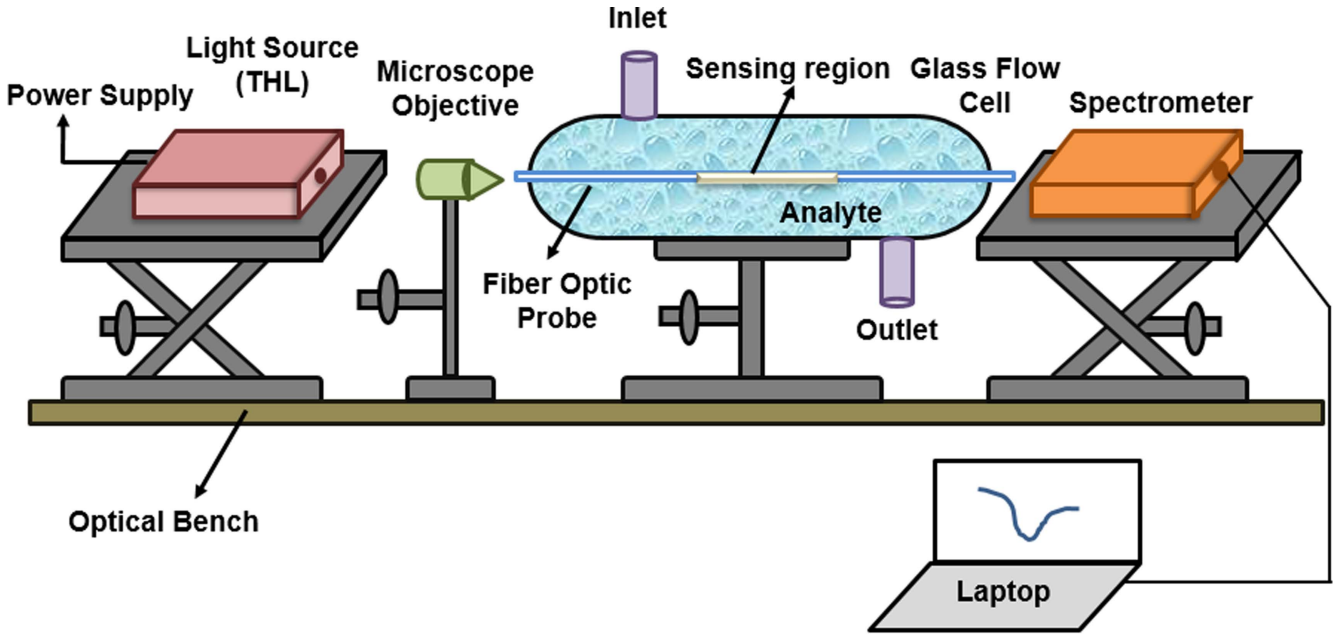

Figure 2. Schematic demonstration of the experimental setup used for the characterization of the fabricated caffeine sensor.

and pH 7. Sample solutions of caffeine in the concentration range from 0 to 500 nM to be used for the characterization of the fabricated sensing probe were prepared in the phosphate buffer solution. A stock solution of caffeine of 500 nM concentration was prepared by dissolving 0.0485 mg of caffeine in 500 ml phosphate buffer. The caffeine solutions of desired concentrations were prepared by appropriate dilution of the stock solution with phosphate buffer. The refractive index of all the prepared solutions was measured using Abbe refractometer and was found to be the same within the accuracy of the refractometer (0.001). To study the influence of pH caffeine solutions of 500 nM concentration and varying pH were prepared in phosphate buffer.

2.5. Experimental setup

The experimental arrangement for the characterization of fabricated fiber optic caffeine sensor is depicted in figure 2. The probe was fixed in a glass flow cell having the provision of insertion and removal of analyte solutions. Unpolarized light from a tungsten halogen lamp (Ava-Light-HAL) was launched into one end of the sensing probe with the help of a microscope objective. At the other end of the fiber, a spectrometer (Avaspec-3648) interfaced with a laptop was placed to record the spectrum of the transmitted light. The output end of the fiber optic probe was placed in close proximity with the entrance slit of the spectrometer so as to achieve the maximum power output which is observed in the laptop interfaced with the spectrometer. It is important to mention that the spectrometer does not measure the far field output of the fiber optic probe as the probe is kept close to the entrance slit of the spectrometer. The resonance wavelength was determined from the spectrum for every analyte solution.

3. Results and discussion

The sensing mechanism of caffeine by the rGO: chitosan: silica sol gel nanohybrid membrane involves oxidation and reduction processes. The interaction of caffeine molecules with the nanohybrid membrane marks the onset of redox reaction between the two described as four electron-four proton transfer reaction [20, 22, 53–55]. Consequently, the dielectric function of the sensing layer gets modified which is reflected in terms of shift in resonance wavelength. The lower content of functional groups containing oxygen atoms and comparatively huge conjugated structures of rGO provides a favorable environment for the charge transfer processes between caffeine and rGO: chitosan: silica sol gel nanohybrid membrane enabling an efficient detection of caffeine. Additionally, the high specific surface area and excellent biocompatibility of rGO combined with an appropriate supporting network provided by chitosan modified silica sol gel imparts large number of adsorption sites and hence a conducive framework for a productive interaction with caffeine molecules.

3.1. Optimization of the sensing probe

Before finalizing the probe for the best performance various fabrication parameters were optimized. The optimization of the fabricated sensing probe was realized in terms of the shift acquired in resonance wavelength during SPR measurements for the change in concentration of caffeine solution from 0 to 500 nM for various fabrication parameters as described in following subsections.

3.1.1. Concentration of rGO encapsulated in chitosan modified silica sol gel. The concentration of rGO being encapsulated in hybrid polymer network of chitosan modified silica sol gel

is an important factor to be considered during fabrication as it determines the degree of interaction of caffeine molecules with the sensing layer. An optimum rGO concentration that can be held in the polymer matrix leads to an efficient interaction of caffeine molecules with the sensing surface and hence an increase in sensitivity. Nanohybrid membranes with varying concentration of rGO were synthesized and dip coated over the fiber optic sensing probes. For this, the probe was kept in the solution of rGO: chitosan: silica sol gel nanohybrid membrane for 9 min before pulling. The shift in resonance wavelength attained for each of the probes for the change in caffeine concentration from 0 to 500 nM (pH 7) is plotted in figure 3(a). It is noted that the maximum shift in resonance wavelength is achieved for 15 mM rGO concentration. Since the shift in resonance wavelength is correlated to the sensitivity of the sensor, it is concluded that the sensing probe coated with 15 mM rGO concentration encapsulated in the polymer network is highly sensitive towards caffeine. A morphological investigation of the rGO: chitosan: silica sol gel nanohybrid membrane with different rGO concentrations, 0, 5, 10, 15, 20 mM, was carried out using scanning electron microscopy (SEM) and are displayed in figure 3(b)(i–v). It is revealed from SEM micrographs that the nanohybrid membrane in all the cases is composed of rGO encapsulated in chitosan modified silica sol gel. The dielectric function of the nanohybrid membrane is largely influenced by the concentration of rGO. For low rGO concentration, the amount of shift in resonance wavelength obtained is small as there are not enough rGO molecules to interact with the caffeine molecules. On increasing the concentration of rGO, the shift in resonance wavelength achieved also increases due to an efficient interaction of caffeine molecules with the nanohybrid membrane forming the sensing channel. However, on further increasing rGO concentration, the amount of shift reduces as an excess of rGO concentration gets imperfectly encapsulated in the polymer matrix of chitosan modified silica sol gel as it can confine only a limited amount of rGO. This reduces an efficient interaction of caffeine molecules with the sensing layer and thus, the shift attained in SPR spectra starts decreasing. Thus, the optimized concentration of rGO in the polymer matrix is 15 mM. Figure 3(c) shows SEM image of completely fabricated fiber optic sensing probe with the optimized concentration of rGO encapsulated in the polymer matrix.

3.1.2. Dipping time of Ag coated probe in solution of rGO: chitosan: silica sol gel nanohybrid membrane. The next optimization parameter is the dipping time of the silver coated probe in the solution of rGO: chitosan: silica sol gel nanohybrid membrane before pulling as it decides the thickness of the sensing layer being deposited over the silver coated core region of the probe. An optimum thickness of the sensing layer is responsible for an effective interaction of the analyte molecules with the sensing layer and hence an efficient generation of SPR signal. Here, the silver coated probes were dipped in solution of nanohybrid membrane of rGO: chitosan: silica sol gel with rGO concentration of 15 mM for different times before pulling using the dip coating technique. Figure 4(a) displays the shift in resonance wavelength obtained for the change in concentration of caffeine from 0 to 500 nM for different dipping times of the probe in solution of nanohybrid membrane. It is noticed that the shift in resonance wavelength first increases with an increase in dipping duration, acquires a maximum for dipping duration of about 9 min and then starts decreasing. The observed trend is explained on the basis that for smaller dipping durations, a thin and less stable sensing layer gets deposited on the fiber optic probe which leads to smaller shift in resonance wavelength. Also, for longer dipping durations, the sensing layer gets roughened up and becomes thick enough and reaches the limit up to which the evanescent field can penetrate and interact with the analyte molecules resulting in generation of SPR signal. The thickness of the sensing layer deposited with dipping duration of 9 min was evaluated through optical profilometer. For this, rGO: chitosan: silica sol gel nanohybrid membrane layer was deposited using 9 min dipping period over the glass slide substrate. Figure 4(b) shows the optical spectrum obtained using profilometer for the film deposited over the substrate. The thickness of the film from the spectrum was determined from the average of the height difference between the red and green spots and the blue and green spots. The height difference between the red and green spots obtained from the spectrum is 992.3 nm and that between the blue and green spots is 862.8 nm. The average of these two values, taken as the film thickness, comes out to be 927.6 nm. This can be taken as an optimum value of film thickness which leads to the maximum shift in the resonance wavelength and hence maximum sensitivity of the sensor.

3.2. Influence of pH of buffer solution

The effect of pH of the buffer solution used for making analyte solutions over the performance of the sensor has been examined to elucidate the sensitivity of the sensor at different pH of the sample solution. To explore this, SPR studies were carried out on caffeine solutions 0 and 500 nM concentrations prepared in phosphate buffer of varying pH value. Figure 5 shows the variation of shift in resonance wavelength attained for different pH values of the phosphate buffer. It may be noted from the figure that the maximum shift in resonance wavelength occurs when the pH of buffer solution is 7. Therefore, it is inferred that the sensor shows its best performance at pH 7 and displays maximum sensitivity at this pH value.

3.3. Characterization of the probe through SPR studies

The characterize the optimized probe fabricated with 15 mM rGO concentration and 9 min of dipping period caffeine solutions of concentration 0–500 nM and pH 7 were introduced into the flow cell consecutively and their respective SPR spectra were recorded which are shown in figure 6(a). A shift of resonance wavelength towards higher wavelength regime is observed with an increase in the caffeine

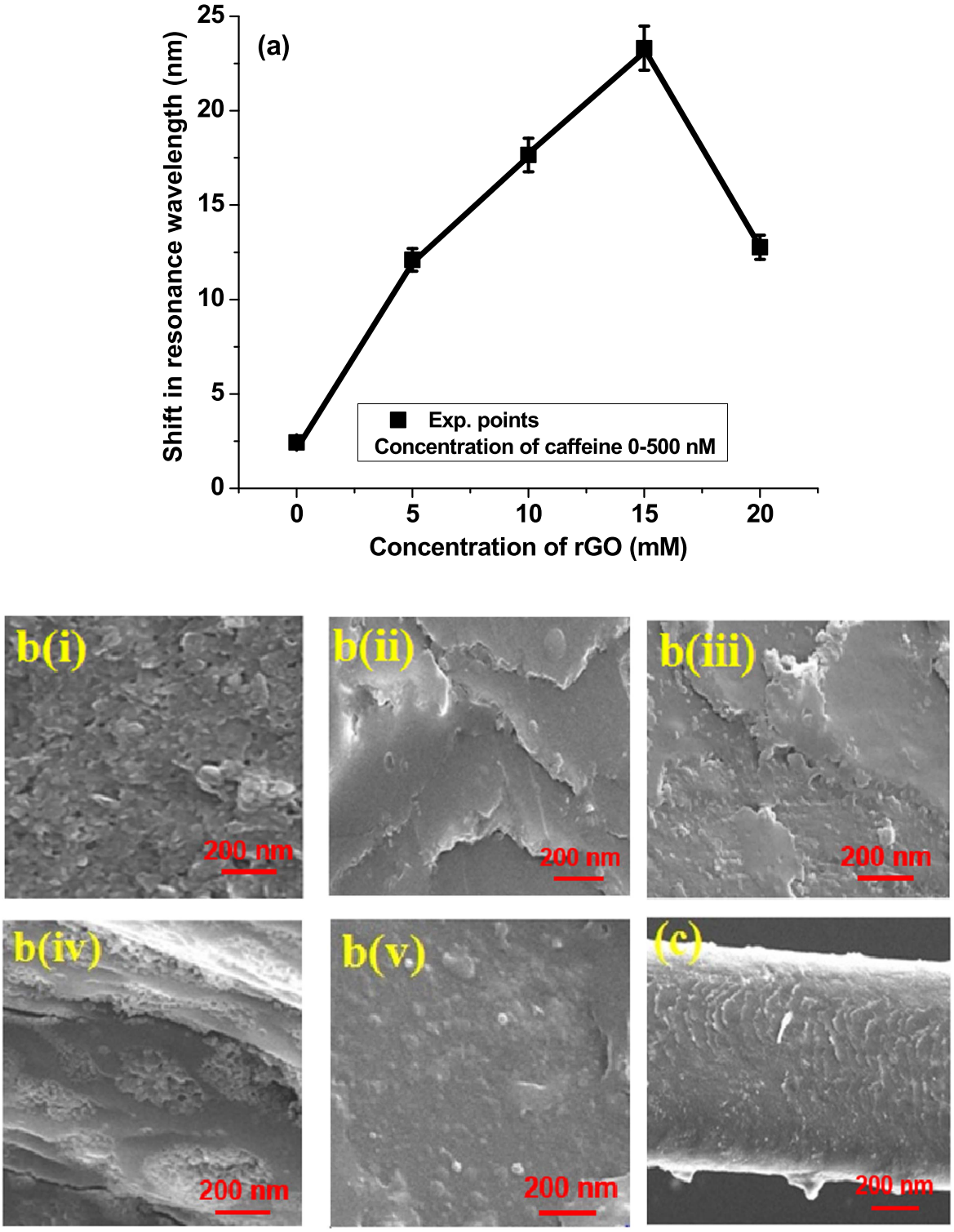

Figure 3. (a) Variation of shift in resonance wavelength attained with rGO concentration for optimization of rGO concentration encapsulated in polymer network of chitosan and silica sol gel, (b) SEM images of the synthesized rGO: chitosan: silica sol gel nanohybrid membrane over glass substrate with different concentration of rGO: (i) 0 mM; (ii) 5 mM; (iii) 10 mM; (iv) 15 mM; (v) 20 mM, (c) SEM image of the fiber optic sensing probe with 15 mM rGO concentration in polymer network of chitosan and silica sol gel.

concentration. The trend is justified based on interaction of caffeine molecules with rGO: chitosan: silica sol gel nanohybrid membrane resulting in an alteration of the dielectric function of the nanohybrid membrane as explained above. The interaction modifies both the real and the imaginary parts of the complex dielectric function of the sensing surface. While the modification in real part of dielectric function accounts for the wavelength shift, the change in the imaginary part explains the observed variation in the depth of SPR curves corresponding to varied caffeine concentration values.

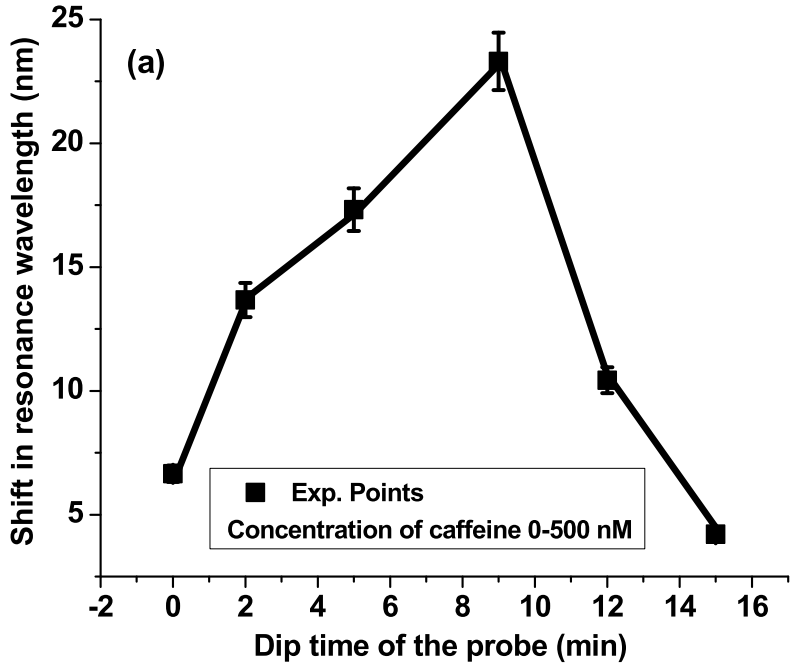

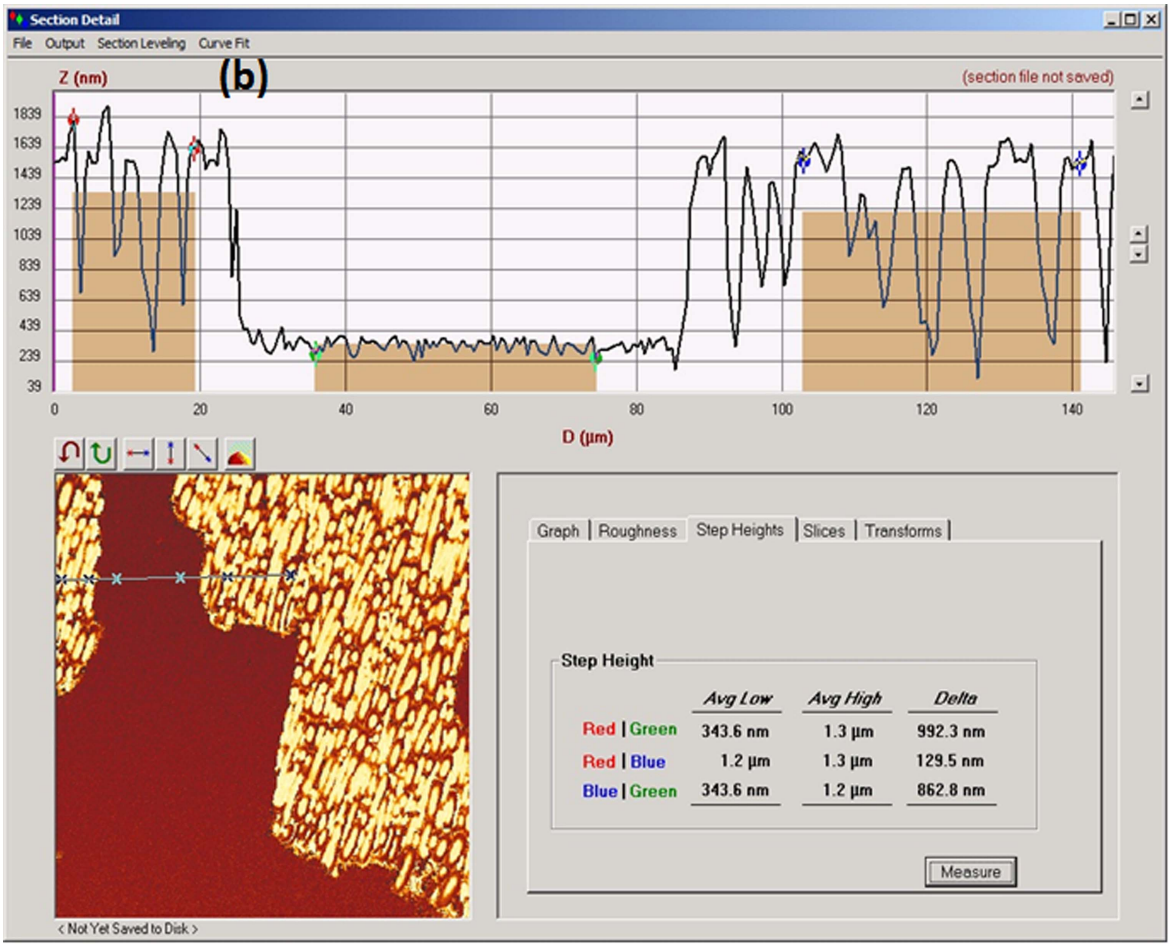

Figure 4. (a) Variation of shift in resonance wavelength achieved with dip time of silver coated probe in solution of rGO: chitosan: silica sol gel nanohybrid membrane, (b) optical profilometer spectrum to estimate the thickness of rGO: chitosan: silica sol gel nanohybrid membrane deposited over glass slide substrate.

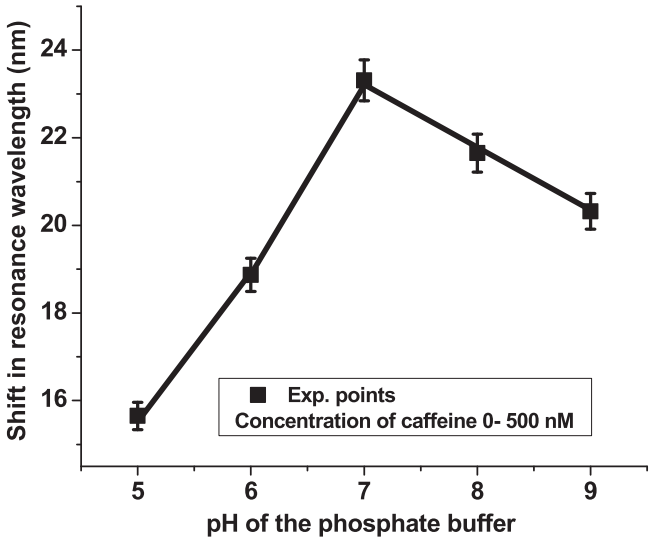

Figure 5. Variation of shift in resonance wavelength acquired with different pH values of the buffer solution used for preparing caffeine solutions.

The numeric values of resonance wavelengths obtained from SPR curves of figure 6(a) for each concentration value of caffeine have been plotted in figure 6(b) as a function of caffeine concentration. This is termed as the calibration curve of the sensor. Here the points corresponding to the resonance wavelength values have been fitted which follow an exponentially increasing fashion with the concentration of caffeine. The experiments were performed four times for each of the analyte concentration values and the four values of resonance wavelength were recorded from their SPR spectra. The variance of each set of resonance wavelength values was calculated using following relation

$$\mathrm{Var} = \frac{1}{4}\sum_{i=1}^{4}(\lambda_{\mathrm{m}} - \lambda_i)^2, \qquad (1)$$

where λ_{m} represents the mean of the recorded values of resonance wavelength (λ_i). The square root of the variance thus obtained gave the standard deviation in resonance wavelength for a particular concentration of the analyte. In a similar manner, standard deviation values were determined for all the concentrations of caffeine which have been plotted as error bars in figure 6(b). Sensitivity of the sensor is defined as the change in resonance wavelength per unit change in analyte concentration and is calculated from the slope of the calibration curve. Quantitatively, sensitivity is determined by differentiating the exponential obtained in the calibration curve. Figure 6(c) depicts the variation of sensitivity values thus achieved with the concentration of caffeine. The error bars shown in the figure were determined using the above method. It is noted that the sensitivity curve follows a declining trend within the entire range of caffeine concentration. This is explained on the grounds that the continual exposure of the sensing probe to analyte molecules results in diminishing the active sites in the sensing layer to efficiently

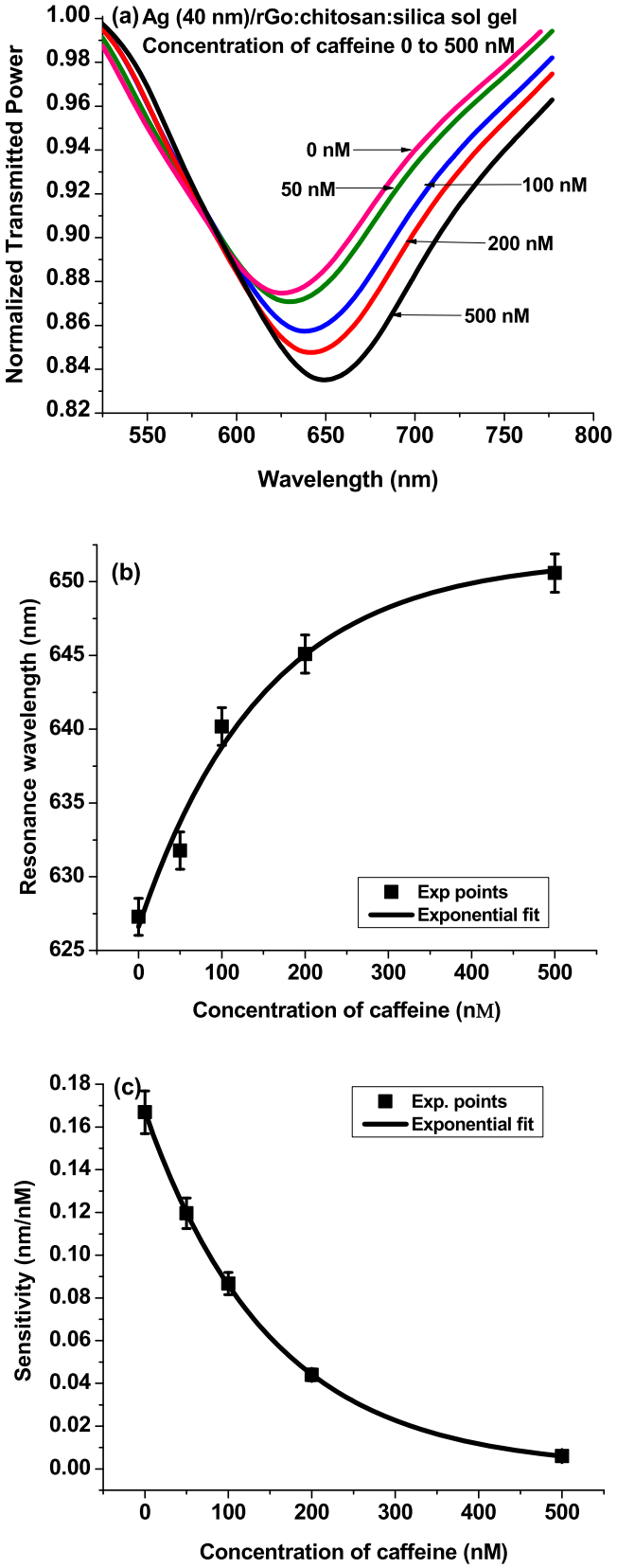

Figure 6. (a) Experimental SPR spectra of the probe with multilayers of Ag and rGO/silica sol gel nanohybrid membrane for 0–500 nM concentration range of caffeine in the vicinity of the sensing region, (b) variation of resonance wavelength with caffeine concentration, (c) variation of sensitivity with caffeine concentration.

Table 1. Comparison of the proposed fiber optic SPR caffeine sensor with several other sensors reported in the literature with different sensing methodologies.

Sensing methodology	LOD (μM)	References
HPLC	9.78	[8]
Liquid chromatography-tandem mass spectrometry	1.25	[10]
Electrochemical using bare boron-doped diamond electrode	0.15	[11]
Square wave voltammetry	0.79	[12]
Amperometry using core–shell Cu_2O nanocubes enfolded with $Co(OH)_2$ on rGO	0.4	[13]
Fluorescence	51.5	[14]
Spectrophotometry	1.545	[15]
Stepwise injection analysis with potentiometric detection	6	[16]
Electrospray ionization ion mobility spectrometry	1.03	[17]
Electrochemical	0.137	[21]
Piezoelectric quartz sensor	0.0027	[56]
FOSPR and Ag/rGO: chitosan: silica sol gel	0.001994 (0.002)	Present study

interact with the analyte molecules and hence a reduction in sensitivity is observed.

The sensitivity value near zero concentration of analyte is used to calculate an important performance parameter of the sensor, namely, limit of detection (LOD), mathematically expressed as [30]

$$\mathrm{LOD} = \frac{\Delta\lambda}{S_{C=0}}, \tag{2}$$

where $\Delta\lambda$ represents the resolution of the spectrometer and $S_{C=0}$ is the sensitivity near zero analyte concentration. For this case, $\Delta\lambda = 0.333$ nm and $S_{C=0} = 0.167\ \mathrm{nm\,nM^{-1}}$ as determined from figure 6(c). These values provide LOD of the present caffeine sensor as 1.994 nM. A comparison of the achieved LOD value with the LOD values reported in the literature using different detection schemes and tabulated in table 1 reveals that the LOD of the proposed sensor is minimum, which makes the present sensor superior to previously reported ones.

3.4. Response time and repeatability

The response time and repeatability of the fabricated sensor have been determined through SPR measurements conducted on 50 nM concentration (pH 7) solution of caffeine. Initially, the transmitted power at 630 nm wavelength was recorded in the absence of caffeine solution in the flow cell. Thereafter, the transmitted power was recorded after 1 min of insertion of caffeine solution and was observed to decrease. No change in the transmitted power was observed when it was again recorded after 1 min implying that the response time of the sensor is less than a minute. The cycle of measurement was completed by recording the transmitted power after complete removal of caffeine solution from the flow cell which was found to be almost equal to the initial value. This operation was repeated several times and the results are depicted in figure 7(a) for two cycles. A negligible variation in the values of transmitted power for zero and 50 nM concentration at 630 nm wavelength implies that the sensor possesses good repeatability. To estimate the value of response time of the sensor more accurately experiments were performed with much faster sampling rate. Figure 7(b) depicts the time response of the normalized transmitted power in the absence and just after adding caffeine solution (50 nM, pH 7) in the glass flow cell. As is observed, the transmitted power first

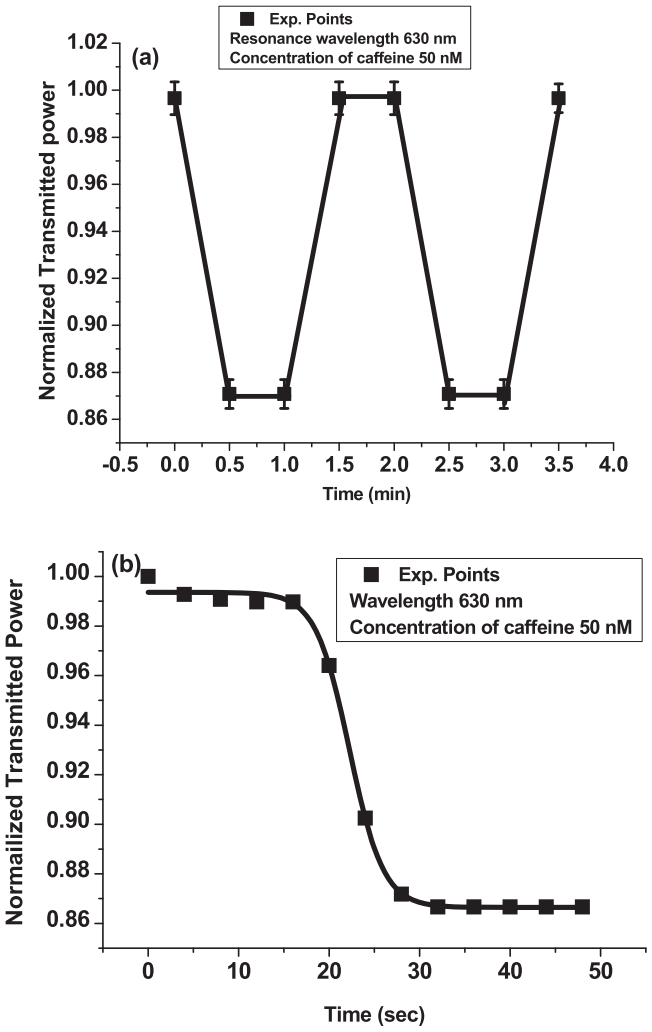

Figure 7. (a) Repeatability test of the fabricated caffeine sensor for 0–50 nM caffeine concentration, and (b) time response of the sensor just after adding caffeine sample of 50 nM in the flow cell.

decreases and saturates after approximately 16 s. Thus, the response time of the sensor is deduced to be 16 s.

4. Conclusion

In the present study, we have designed, fabricated and characterized a SPR based fiber optic caffeine sensor. For this purpose, a nanohybrid membrane of rGO encapsulated in polymer matrix of chitosan and silica sol gel was synthesized adopting chemical route and characterized through SEM studies and profilometer spectrum. The optical response characteristics of the fabricated sensor analyzed via SPR measurements in wavelength interrogation module revealed a red shift in resonance wavelength with an increase in caffeine concentration around the sensing region of the probe. The optimum concentration of rGO in polymer network of chitosan and silica sol gel as well as the optimum dipping time of the probe in the solution of nanohybrid membrane of rGO: chitosan: silica sol gel were figured out to obtain the best performance of the sensor. SPR measurements on the optimized sensing probe concluded that the sensor has high sensitivity, wide operating range and good reproducibility indicating that rGO: chitosan: silica sol gel nanohybrid membrane could be a promising option for the development of a potential detection protocol for caffeine. A comparison of the attained LOD value with the earlier reported LOD values using different sensing protocols further unveils the superiority of the present work over others. Finally, the synergistic combination and the concomitant advantages of surface plasmon resonance and fiber optics confirm the prospects of the present sensor for commercial applications for caffeine detection in biological fluids, various foodstuffs and pharmaceutical formulations.

Acknowledgments

Ravi Kant is grateful to Council of Scientific and Industrial Research (CSIR), India for providing research fellowship. Rana Tabassum is thankful to Department of Science and Technology (DST), India for INSPIRE fellowship.

References

[1] Nathanson J A 1984 Caffeine and related methylxanthines: possible naturally occurring pesticides *Science* **226** 184–7
[2] Derry C J, Derry S and Moore R A 2012 Caffeine as an analgesic adjuvant for acute pain in adults *Cochrane Database Syst. Rev.* **14** CD009281
[3] Vichare V, Mujgond P, Tambe V and Dhole S N 2010 Simultaneous spectrophotometric determination of paracetamol and caffeine in tablet formulation *Int. J. Pharm Tech. Res.* **2** 2512–6
[4] Nawrot P, Jordan S, Eastwood J, Rotstein J, Hugenholtz A and Feeley M 2003 Effects of caffeine on human health *Food Addit. Contam.* **20** 1–30
[5] Verhoef P, Pasman W J, Van Vliet T, Urgert R and Katan M B 2002 Contribution of caffeine to the homocysteine-raising effect of coffee: a randomized controlled trial in humans *Am. J. Clin. Nutr.* **76** 1244–8
[6] Kuranda K, Leberre V, Sokol S, Palamarczyk G and François J 2006 Investigating the caffeine effects in the yeast Saccharomyces cerevisiae brings new insights into the connection between TOR, PKC and Ras/cAMP signalling pathways *Mol. Microbiol.* **61** 1147–66
[7] Tripathi A, Tiwari B, Patil R, Khanna V and Singh V 2015 The role of salivary caffeine clearance in the diagnosis of chronic liver disease *J. Oral. Biol. Craniofac. Res.* **5** 28–33
[8] Fernández P L, Martín M J, González A G and Pablos F 2000 HPLC determination of catechins and caffeine in tea. Differentiation of green, black and instant teas *Analyst* **125** 421–5
[9] Srdjenovic B, Djordjevic-Milic V, Grujic N, Injac R and Lepojevic Z 2008 Simultaneous HPLC determination of caffeine, theobromine, and theophylline in food, drinks, and herbal products *J. Chromatogr. Sci.* **46** 144–9
[10] Ptolemy A S, Tzioumis E, Thomke A, Rifai S and Kellogg M 2010 Quantification of theobromine and caffeine in saliva, plasma and urine via liquid chromatography-tandem mass spectrometry: a single analytical protocol applicable to cocoa intervention studies *J. Chromatography* B **878** 409–16
[11] Švorc L, Tomčík P, Svítková J, Rievaj M and Bustin D 2012 Voltammetric determination of caffeine in beverage samples on bare boron-doped diamond electrode *Food Chem.* **135** 1198–204
[12] Tefera M, Geto A, Tessema M and Admassie S 2016 Simultaneous determination of caffeine and paracetamol by square wave voltammetry at poly(4-amino-3-hydroxynaphthalene sulfonic acid)-modified glassy carbon electrode *Food Chem.* **210** 156–62
[13] Velmurugan M, Karikalan N, Chen S and Karuppiah C 2016 Core–shell like Cu_2O nanocubes enfolded with $Co(OH)_2$ on reduced graphene oxide for the amperometric detection of caffeine *Microchim. Acta* **183** 2713–21
[14] Nanjundaiah S, Krishna H and Bhatt P 2016 Fluorescence based turn-on probe for the determination of caffeine using europium-tetracycline as energy transfer complex *J. Fluorescence* **26** 1115–21
[15] Xia Z, Ni Y and Kokot S 2013 Simultaneous determination of caffeine, theophylline and theobromine in food samples by a kinetic spectrophotometric method *Food Chem.* **141** 4087–93
[16] Timofeeva I, Medinskaia K, Nikolaeva L, Kirsanov D and Bulatov A 2016 Stepwise injection potentiometric determination of caffeine in saliva using single-drop microextraction combined with solvent exchange *Talanta* **150** 655–60
[17] Jafari M T, Rezaei B and Javaheri M 2011 A new method based on electrospray ionisation ion mobility spectrometry (ESI-IMS) for simultaneous determination of caffeine and theophylline *Food Chem.* **126** 1964–70
[18] Peri-Okonny U L, Wang S X, Stubbs R J and Guzman N A 2005 Determination of caffeine and its metabolites in urine by capillary electrophoresis-mass spectrometry *Electrophoresis* **26** 2652–63
[19] Sanghavi B J and Srivastava A K 2010 Simultaneous voltammetric determination of acetaminophen, aspirin and caffeine using an *in situ* surfactant-modified multiwalled carbon nanotube paste electrode *Electrochim. Acta* **55** 8638–48
[20] Sun J Y, Huang K J, Wei S Y, Wu Z W and Ren F P 2011 A graphene-based electrochemical sensor for sensitive determination of caffeine *Colloids Surf.* B **84** 421–6

[21] Amare M and Admassie S 2012 Polymer modified glassy carbon electrode for the electrochemical determination of caffeine in coffee *Talanta* **93** 122–8

[22] Xiong X Q, Huang K J, Xu C X, Jin C X and Zhai Q G 2013 Glassy carbon electrode modified with poly(taurine)/TiO_2–graphene composite film for determination of acetaminophen and caffeine *Chem. Ind. Chem. Eng. Q.* **19** 359–68

[23] Yanase Y, Araki A, Suzuki H, Tsutsui T, Kimura T, Okamoto K, Nakatani T, Hiragun T and Hide M 2010 Development of an optical fiber SPR sensor for living cell activation *Biosens. Bioelectron.* **25** 1244–7

[24] Kim S A, Kim S J, Moon H and Jun S B 2012 *In vivo* optical neural recording using fiber-based surface plasmon resonance *Opt. Lett.* **37** 614–6

[25] Pollet J, Delport F, Janssen K P, Jans K, Maes G, Pfeiffer H, Wevers M and Lammertyn J 2009 Fiber optic SPR biosensing of DNA hybridization and DNA-protein interactions *Biosens. Bioelectron.* **25** 864–9

[26] Homola J, Yee S S and Gauglitz G 1999 Surface plasmon resonance sensors: review *Sensors Actuators* B **54** 3–15

[27] Gupta B D, Srivastava S K and Verma R 2015 *Fiber Optic Sensors Based on Plasmonics* (Singapore: World Scientific)

[28] Anker J N, Hall W P, Lyandres O, Shah N C, Zhao J and Duyne R P V 2008 Biosensing with plasmonic nanosensors *Nat. Mater.* **7** 442–53

[29] Colson P, Henrist C and Cloots R 2013 Nanosphere lithography: a powerful method for the controlled manufacturing of nanomaterials *J. Nanomater.* **2013** 948510

[30] Tabassum R, Kaur P and Gupta B D 2016 Tuning the field distribution and fabrication of an Al@ZnO core–shell nanostructure for a SPR-based fiber optic phenyl hydrazine sensor *Nanotechnology* **27** 215501

[31] Kant R, Tabassum R and Gupta B D 2017 A highly sensitive and distinctly selective d-sorbitol biosensor using SDH enzyme entrapped Ta_2O_5 nanoflowers assembly coupled with fiber optic SPR *Sensors Actuators* B **242** 810–7

[32] Geim A K and Novoselov K S 2007 The rise of graphene *Nat. Mater.* **6** 183–91

[33] Li D and Kaner R B 2008 Graphene-based materials *Science* **320** 1170–1

[34] Navaee A, Salimi A and Teymourian H 2012 Graphene nanosheets modified glassy carbon electrode for simultaneous detection of heroine, morphine and noscapine *Biosens. Bioelectron.* **31** 205–11

[35] Xia F, Farmer D B, Lin Y M and Avouris P 2010 Graphene field-effect transistors with high on/off current ratio and large transport band gap at room temperature *Nano Lett.* **10** 715–8

[36] Yoo J J *et al* 2011 Ultrathin planar graphene supercapacitors *Nano Lett.* **11** 1423–7

[37] Cracknell J A, Vincent K A and Armstrong F A 2008 Enzymes as working or inspirational electrocatalysts for fuel cells and electrolysis *Chem Rev.* **108** 2439–61

[38] Becerril H A, Mao J, Liu Z, Stoltenberg R M, Bao Z and Chen Y 2008 Evaluation of solution-processed reduced graphene oxide films as transparent conductors *ACS Nano* **2** 463–70

[39] Eda G, Fanchini G and Chhowalla M 2008 Large-area ultrathin films of reduced graphene oxide as a transparent and flexible electronic material *Nat. Nanotechnol.* **3** 270–4

[40] Eda G and Chhowalla M 2010 Chemically derived graphene oxide: towards large-area thin-film electronics and optoelectronics *Adv. Mater.* **22** 2392–415

[41] Welch C M and Compton R G 2006 The use of nanoparticles in electroanalysis: a review *Anal. Bioanal. Chem.* **384** 601–19

[42] Zhou M, Zhai Y and Dong S 2009 Electrochemical sensing and biosensing platform based on chemically reduced graphene oxide *Anal. Chem.* **81** 5603–13

[43] Wei J, Qiu J, Li L, Ren L, Zhang X, Chaudhuri J and Wang S 2012 A reduced graphene oxide based electrochemical biosensor for tyrosine detection *Nanotechnology* **23** 335707

[44] Zhou X H, Liu L H, Bai X and Shi H C 2013 A reduced graphene oxide based biosensor for high-sensitive detection of phenols in water samples *Sensors Actuators* B **181** 661–7

[45] Yang Y, Asiri A M, Du D and Lin Y 2014 Acetylcholinesterase biosensor based on a gold nanoparticle–polypyrrole–reduced graphene oxide nanocomposite modified electrode for the amperometric detection of organophosphorus pesticides *Analyst* **139** 3055–60

[46] Agnihotri N, Chowdhury A D and De A 2015 Non-enzymatic electrochemical detection of cholesterol using β-cyclodextrin functionalized graphene *Biosens. Bioelectron.* **63** 212–7

[47] Li D W, Luo L, Lv P F, Wang Q Q, Lu K Y, Wei A F and Wei Q F 2016 Synthesis of polydopamine functionalized reduced graphene oxide-palladium nanocomposite for laccase based biosensor *Bioinorg. Chem. Appl.* **2016** 5360361

[48] Palanisamy S, Thirumalraj B, Chen S M, Wang Y T, Velusamy V and Ramaraj S K 2016 A facile electrochemical preparation of reduced graphene oxide@polydopamine composite: a novel electrochemical sensing platform for amperometric detection of chlorpromazine *Sci. Rep.* **6** 33599

[49] Tsionsky M, Gun G, Giezer V and Lev O 1994 Sol-gel-derived ceramic-carbon composite electrodes: introduction and scope of applications *Anal. Chem.* **66** 1747–53

[50] Liu X, Xie L and Li H 2012 Electrochemical biosensor based on reduced graphene oxide and Au nanoparticles entrapped in chitosan/silica sol–gel hybrid membranes for determination of dopamine and uric acid *J. Electroanal. Chem.* **682** 158–63

[51] Stankovich S, Dikin D A, Piner R D, Kohlhaas K A, Kleinhammes A, Jia Y, Wu Y, Nguyen S T and Ruof R S 2007 Synthesis of graphene-based nanosheets via chemical reduction of exfoliated graphite oxide *Carbon* **45** 1558–65

[52] Fontana E 2006 Thickness optimization of metal films for the development of surface-plasmon-based sensors for nonabsorbing media *Appl. Opt.* **45** 7632–42

[53] Khoo W Y H, Pumera M and Bonanni A 2013 Graphene platforms for the detection of caffeine in real samples *Anal. Chim. Acta* **804** 92–7

[54] Raj M A and John S A 2013 Simultaneous determination of uric acid, xanthine, hypoxanthine and caffeine in human blood serum and urine samples using electrochemically reduced graphene oxide modified electrode *Anal. Chim. Acta* **771** 14– 20

[55] Kesavan S, Raj M A and John S A 2016 Formation of electrochemically reduced graphene oxide on melamine electrografted layers and its application toward the determination of methylxanthines *Anal. Biochem.* **496** 14–24

[56] Ebarvia B S and Sevilla F 2005 Piezoelectric quartz sensor for caffeine based on molecularly imprinted polymethacrylic acid *Sensors Actuators* B **107** 782–90